



Integrated electrocoagulation–photoelectrocatalytic oxidation for effective treatments of aqueous solution bisphenol-A using green-synthesized ZnO nanoparticles

Maruthamuthu Govindaraj¹ · Sham Babu² · Ramasamy Rathinam³ · Vijayan Vasini⁴ · Kaliyapillai Vijayakumar⁵

Received: 11 April 2022 / Accepted: 5 September 2022 / Published online: 14 September 2022
© Institute of Chemistry, Slovak Academy of Sciences 2022

Abstract

In the present investigation, a combined approach of electrocoagulation followed by photoelectrocatalytic oxidation of aqueous bisphenol-A (BPA) solution using titanium electrode coated by mixed metal oxides ($\text{RuO}_2/\text{IrO}_2/\text{TaO}_2$) through green-synthesized ZnO nanocatalyst (NPs) was performed. The biosynthesized RF-ZnO NPs were confirmed as nanoparticles using UV–Vis, FTIR spectroscopy, BET analysis, SEM, EDAX, HR-TEM, and XRD analysis. In the primary treatment process, the aqueous BPA solution was treated by electrocoagulation. The efficient ZnO NPs photocatalytic agent was synthesized from *Rubus fairholmianus* root extract. The removal of BBA was achieved at 59.83% at 20 min of treatment time. After completion of the electrocoagulation process, a secondary treatment process of photoelectrocatalytic oxidation with different operating parameters was investigated. The complete mineralization of BBA could be attained at a 25 mA cm^{-2} of current density at treatment time of 90 min by photoelectrocatalytic oxidation. With an aid of supporting electrolyte (NaCl) in the basic medium, BPA degradation rates were increased with increasing applied current. GC–MS analysis was used to investigate the by-products obtained by degradation and the results were matched with standard NIST database. The kinetic parameters for degradation were calculated, which were fitted well with the pseudo-first-order kinetic model.

Keywords Endocrine-disrupting chemicals · Bisphenol-A (BPA) · Integrated treatment · Electrocoagulation (EC) · Photoelectrocatalytic (PEC) oxidation · Biosynthesized RF-ZnO nanoparticles (RF-ZnO NPs)

Introduction

Bisphenol-A [BPA; 2,2-bis(4-hydroxyphenyl) propane] is a familiar endocrine disruptor in humans and an emerging toxin in diverse environmental compartments (Kang et al.

2006; Laxma et al. 2018). BPA is greatly employed as the raw candidate to produce polysulphonate and phenol resins, unsaturated polyesters, and polyacrylates, nevertheless chiefly to generate epoxy resins and polycarbonate plastics (Govindaraj et al. 2012; Abdul et al. 2021). The epoxy resins are used in aerospace applications, automobile parts, adhesives, metal jar lids, a coating for PVC pipe, and electrical and electronic equipment. Polycarbonate plastics are used in manufacturing automotive lenses, dental sealants, household appliances, rubber chemicals, CDs, DVDs, food packaging, and plastic bottles (Kang et al. 2006; Govindaraj et al. 2013).

BPA is commonly found in environmental concentrations that vary considerably from ng/L level to g/L level by leaching from final products and some manufacturing industrial effluents. BPA has low biodegradability and recalcitrance, necessitating the development of an effectual technique for removing BPA from water (Abdul et al. 2021). Conventional treatment methods have been utilized to treat BPA, including chemical, electrochemical oxidation, photocatalytic degradation, and biological processes. Consequently, it is urgent to

✉ Maruthamuthu Govindaraj
govindarajm.sh@krct.ac.in; mgrajchemist@gmail.com

¹ Department of Chemistry, K.Ramakrishnan College of Technology (Autonomous), Samayapuram, Tiruchirappalli, Tamil Nadu 621112, India

² Department of Mechanical Engineering, PSG College of Technology (Autonomous), Coimbatore, Tamil Nadu 641 004, India

³ Department of Chemistry, Sri Eshwar College of Engineering, Coimbatore, Tamil Nadu 641202, India

⁴ Department of Botany, Kongunadu Arts and Science College (Autonomous), Coimbatore, Tamil Nadu 641 029, India

⁵ Department of Chemistry, M.Kumarasamy College of Engineering, Karur, Tamil Nadu 639 113, India

find out a harmless, facile, and potential treatment technique to remove or degrade BPA (Goulart et al. 2019).

Nidheesh et al. (2021) have applied combination electrocoagulation degradation procedures to successfully treat various contaminants in wastewater. In a variety of organic and inorganic contaminants, the performance of the electrocoagulation approach combined with degrading treatment was reported. In our previous study, the effectiveness and feasibility of the processes to treat BPA aqueous solution by hybrid electrocoagulation subsequently by electrochemical oxidation techniques were evaluated (Govindaraj and Pattabhi 2015). The electrocoagulation treatment is demonstrated as a potential wastewater treatment technique and it successfully treats different kinds of pollutants (arsenic, boron, chromium, phosphate, strontium, organic acid, dyes, bacteria, viruses, cysts, etc.), treats various industrial wastes (paper, olive oil, petroleum refinery, pesticides, tannery, dyes, textiles, etc.), and is able to handle fluctuations in pollutant quantity and quality (Kobyta et al. 2011; Govindaraj and Pattabhi 2015; Nidheesh et al. 2021). Photoelectrocatalysis, or photoelectrochemical degradation, is a novel form of electrochemistry that combines the techniques of photocatalysis technologies with the opportunity to disperse electron holes photogenerated ($e/h+$) and to inhibit their recombination with electrochemical oxidation techniques to treat organic pollutants in water and wastewater in an enriched manner (Daghrir et al. 2012; Argote-Fuentes et al. 2021).

Nanotechnology has enormous potential for improving water and wastewater treatment efficiency while also augmenting supply of water supply by means of safe use of alternative water sources (Qu et al. 2013). Zinc oxide (ZnO) has widely recognized *n*-type semiconductor with unique properties such as a 3.3 eV of direct band gap and a large excitation of 60 meV binding energy, which is why it is used as a photocatalyst to degrade diverse pollutants from aqueous medium. The unique characteristics of ZnO nanoparticles and their conjunction with modern treatment approaches facilitate ample openings to develop remediation of polluted waters (Senthilkumar et al. 2017; Majumder et al. 2020). Photoelectrocatalytic (PEC) degradation of numerous organic contaminants has attracted great attention with ZnO nanoparticles immobilized on conductive substrates.

Recently, there has been an emergent requirement to improve environmentally friendly nanoparticle synthesis approaches without using toxic chemicals in the synthesis processes. Nanoparticle synthesis by biological methods using algae, plants, microorganisms, and enzymes has been recommended as an achievable, greener alternative to chemical and physical routes (Azizi et al. 2013). Green synthesis of nanoparticles by using plant extracts is an excellent material in the industrial invention of well-dispersed metal NPs. These gorgeous green approaches are free from shortfalls

related to conventional synthetic protocols because of their eco-friendliness (Moodley et al. 2018). Rajendran et al. 2021; Senthilkumar et al. 2017). Green-synthesized ZnO nanostructures are more efficient, non-toxic, and low-cost in the absorption of a large fraction of the prominent photocatalyst activities to degrade several compounds (Senthilkumar et al. 2017; Rajendran et al. 2021). The present investigation attempted newly to integrate the treatment of electrocoagulation and photoelectrocatalytic oxidation processes into an effective way to treat an aqueous solution. The PEC degradation of BPA takes place on titanium electrode coated with mixed metal oxides ($\text{RuO}_2/\text{IrO}_2/\text{TaO}_2$) and UV light with green-synthesized ZnO nanoparticles simultaneously.

Previously, no study performed the adaptation of hybrid electrocoagulation with photoelectrocatalytic oxidation treatment methods of the emerging pollutant BPA from aqueous solution using titanium (Ti) electrode coated with mixed metal oxides ($\text{RuO}_2/\text{IrO}_2/\text{TaO}_2$) by green-synthesized ZnO NPs from *Rubus fairholmianus* root extracts. The present work is designed to prepare ZnO NPs using *R. fairholmianus* (RF) root extract through a green chemistry approach and the application of degradation of BPA. To facilitate optimal operating conditions, the PEC degradation process was examined under various solution pHs, ZnO dosages, and different current densities. The removal and degradation effectiveness of the processes was determined by analysis of the removal percentage of BBA and degradation rate.

Material and methods

The reagents were analytical grade and used without any purification. A stock solution concentration of 500 mg L^{-1} was prepared by dissolving precisely measured amount of BPA (MerkChem, Mumbai, India) in double-distilled water, and 1 N NaOH was added to enhance solubility (Staples et al. 1998). The experimental solution was made by diluting the BPA stock solution with distilled water to the preferred starting concentration and then adding the various supportive electrolyte concentrations (NaCl). All the glassware used in the experiments was purchased from Borosil (Mumbai, India). All solutions and reagents were prepared using the Millipore Milli-Q system ($> 18.2 \text{ M}\Omega$) of purified water.

Green synthesis of ZnO NPs

Fresh *R. fairholmianus* plant parts were collected from the Avalanchi Range, the Nilgiris, Tamil Nadu, India, for the period October 2021. The collected *R. fairholmianus* parts were recognized and authenticated from (Voucher specimen number BSI/SRC/5/23/2010–11/Tech.1657) Botanical Survey of India (Southern Circle) Coimbatore, Tamil Nadu, India. Green synthesis of NPs by *R. fairholmianus*

plant root has been performed by adopting the method of Zheng et al. (2015). The *R. fairholmianus* root was cleaned by running water to eliminate dust and soil, dried out, and crushed. The roots powder was extracted sequentially by Soxhlet apparatus for 72 h using acetone as a solvent.

The prepared root extract was subjected to dryness at low pressure using a rotary evaporator. Then, the dried extract (1000 mg) was dissolved in 50 mL of 0.5% dimethyl sulphoxide (DMSO). 50 mL of root extract in 0.5% DMSO was mixed with 50 mL of 0.5 M $\text{Zn}(\text{NO}_3)_2 \cdot 4\text{H}_2\text{O}$ (reagent grade) solution and stirred for 48 h at 80 °C. The transformation of reaction solution colour as pale white from brownish yellow subsequent to introducing root extract with zinc nitrate was observed after 48 h that indicate formation of RF-ZnO NPs (Rajendran et al. 2021). After 30 min of centrifugation at 2500 rpm, the pale white precipitate was formed, and it was washed using double-distilled water. Green-synthesized RF-ZnO NPs were gathered and dried in a hot air oven at 40 °C. The biosynthesized RF-ZnO NPs were compared with those laboratory-synthesized using NaOH according to the technique of Zheng et al. (2015).

Biosynthesized RE-ZnO NPs catalyst characterization techniques

To ascertain the stability of green-synthesized RF-ZnO NPs, a double beam UV–Vis spectrophotometer in the 200–800 nm of wavelength range was used (Shimadzu Pharmaspec-1700, Kyoto, Japan). To elucidate chemical and functional groups, Fourier transform infrared spectroscopy (FTIR) was used (Perkin–Elmer PE 1600, MA, USA). For FTIR analysis, the ZnO NPs were prepared in the form of pellets using KBr and analysed 400–4000 cm^{-1} of the spectral range. The RF-ZnO NPs crystalline structure was characterized by X'Pert-Pro, PAN analytical X-ray diffraction diffractometer Model, CuK–2.2 kW Max with Philips PW1729 ($\lambda = 1.5405 \text{ \AA}$ with Cu-K α radiation source of 45 kV/40 mA).

The specific surface area and average pore diameter of ZnO nanoparticles [BET (Brunauer–Emmett–Teller)] were measured by Quantachrome NOVA 1000 (Boynton Beach, FL, USA). The zeta potential analysis was carried out in Zetasizer Nano ZS (Malvern Instruments Ltd., GB). To study the morphology of prepared RF-ZnO NPs, the JEOL 2100 LaB6 instrument was used to perform HR-TEM microscopic analysis. RF-ZnO NPs surface morphology was characterized by FEI QUANTA 200, USA. To understand the element compositions of the RF-ZnO NPs, EDAX (FEI QUANTA 200, USA) analysis was performed.

Electrocoagulation cell

The electrocoagulation treatment was accomplished in an undivided glass cell. Both the anode and the cathode were constituted by aluminium (Al) plates (0.8 cm thickness). The total active anodic surface area of Al plates was 102 cm^2 . Al electrode surfaces were meticulously cleaned using emery sheets, washed with acetone, and immersed for 10 min in a dilute HCl solution. To confirm complete elimination of impurities, the electrode was rinsed by distilled water, continued by rubbing using abrasive paper before and after every experiment. The volume of the vessel was 1.2 L. The solution was subjected to stirring continuously at 250 rpm by magnetic stirrer during the process. Electric power was provided by a regulated DC rectifier. The entire electrode setup was employed on non-conducting wedges attached to bottom plate of the electrocoagulation tank (Govindaraj et al. 2012).

Photoelectrocatalytic oxidation reactor

The photoelectrocatalytic oxidation treatment was conducted with 1250 mL glass reactor (Fig. 1) furnished with a UV lamp having low-pressure mercury arc lamp (15 W, Philips, model TUV, Chennai, India) quartz jacketed immersion having a wavelength of 365 nm, and the electrodes were arranged in a single compartment cylindrical glass cell. An internal light (UV lamp) source was enclosed by a quartz jacket. To control the temperature at $27 \pm 2 \text{ }^\circ\text{C}$, a cooling water circulation bath is connected to the photo reactor. The reactor's top side holder holds the UV lamp, electrodes, gas outlet, and thermometer (Rathinam and Govindaraj 2021). In the photoelectrocatalytic (PEC) oxidation, using titanium electrode coated with $\text{RuO}_2/\text{IrO}_2/\text{TaO}_2$ mixed metal oxides (Titanium and Tantalum Products, Chennai, India), each two of anodes and cathodes were alternatively looped internally to form the anode and cathode assembly, which had a surface area of 106 cm^2 . A gap of 6 mm was kept between anode

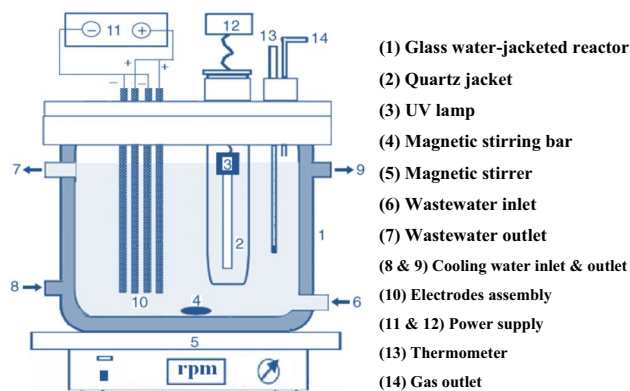


Fig. 1 Schematic diagram of experimental setup for photoelectrocatalytic oxidation reactor

and cathode to minimize the ohmic losses. The electrodes and UV lamp are linked to respective terminals of the regulated DC rectifier. A magnetic stirrer at 250 rpm was used to mix the solution of the PEC reactor during the process. The treated BPA sample was centrifuged at 5000 rpm for 15 min and the supernatant liquid was withdrawn for examination (Rathinam and Govindaraj 2021).

Experimental procedure

Initially, the BPA sample was treated with electrocoagulation at several operating circumstances. The solution pH was optimized using 0.2 M of H_2SO_4 or NaOH. The leads of anode and cathode were joined to individual terminals of the DC rectifier, and electric power was provided by a stabilized power source integrated with a digital ammeter and voltmeter. The solution was stirred continuously at 250 rpm using a magnetic stirrer during the process to allow the chemical precipitate to grow large enough for removal. The centrifugation of the sample was performed at 3000 rpm for 10 min and the supernatant solution was taken for measurement. At the end of the experiment, the power was turned off and the electrodes were detached (Govindaraj and Pattabhi 2015). The experimented aqueous BPA solution was filtered using ordinary filter paper which was subjected to further photoelectrocatalytic (PEC) oxidation process.

For each PEC degradation experiment, 900 mL of the electrocoagulated treated BPA solution was shifted to the photoelectrocatalytic reactor, and a different concentration of RE-ZnO NPs was mixed with the BPA solution. The electrodes were joined to the respective leads of anode and cathode in the DC rectifier and energized for the necessary period at a constant current. The solution was stirred at 250 rpm for continuous mixing during the experiment to confirm the mass transfer efficiency. The progress of PEC degradation of BPA was observed by UV–Vis spectrophotometer (UV-1700 Pharma Spec, Shimadzu UV spectrophotometer, Japan) analysis of treated samples, which were collected at fixed time intervals.

Analytical techniques

The aqueous BPA solution pH and changes in treated solution pH during EC and PEC treatments were checked using a pH meter, which was obtained from Elico Li-120 (Chennai, India). The percentage of BPA value replicates the general organics concentration in solution and had been generally employed to estimate degradation of organic species.

UV–Vis spectra analysis

The BPA removal during electrocoagulation and degradation by photoelectrocatalytic oxidation were measured using

a UV–Vis spectrophotometer (UV–1700 Pharma Spec, Shimadzu, Japan) in a quartz cell between 200 and 800 nm. The characteristic peak was observed at 278 nm for pure BPA.

High-performance liquid chromatography (HPLC) analysis

HPLC (Model–2489, WATERS, USA) equipped with a multiple wavelength UV–visible detector operated at 278 nm was employed to monitor the concentrations of BPA. Separation was accomplished on a reverse phase C18 ($5\ \mu\text{m} \times 250\ \text{mm} \times 4.6\ \text{mm}$) stainless steel column. Acetonitrile 50:50 (v/v) and water mixture was used in the mobile phase that was passed at specified flow rate (1 mL/min) with a volume injection of 10 μL . The detector output was processed with peak empower–2 software. Under these conditions, the retention time (t_r) for BPA was 6.83 min. At the same experimental column condition, the BPA degradation peaks for intermediate compounds were monitored (Ju et al. 2012).

Gas chromatography–mass spectrometry (GC–MS) analysis

Photoelectrocatalytic degradation of BPA intermediates was identified by GC–MS (GC–2010, Shimadzu, Japan) analysis. A 10 ml sample was mixed with 20 ml of dichloromethane (DCM) to extract BPA and intermediates into DCM. The same procedure was done two to three times. After this, they dehydrated the sample using the dehydrating agent anhydrous Na_2SO_4 , concentrated it to almost 5 ml, and retained it at 4 °C. The carrier gas of helium was used through the injection mode of split. GC–MS used a GC furnished with a capillary column (DB-5 ms, $30 \times 0.25\ \text{mm}$, 0.25 m) and a mass spectrometer (MS–QP2010 Plus), which was equipped with an electron ionization (EI) source. The following parameters were employed towards GC–MS analysis to identify BPA intermediates: solvent delay (180 s), split ratio (15:1), oven temperature (50 °C 60 s–300 °C 60 s), scan range (50–500 at 3 scan/s), and ramp rate of 8 °C/min (Abo et al. 2016). The GC–MS data corresponded with the data of reference standard samples compiled by the NIST library and Willey library. The species that matched better than 90% were used for the identification of BPA degradation by-products during the PEC oxidation process.

Calculations

The commercial evaluation of the current technique compared with other methods was calculated with respect to electrical energy consumption at diverse operating conditions by Eq. (1):

$$\text{Energy consumption (kWh/m}^3\text{)} = \frac{UIt_{\text{Ec}}}{\text{Treated volume (L)}} \quad (1)$$

where U is cell voltage in volts (V), I is current in amperes (A), and t_{Ec} is time of electrocoagulation process per hour (El-Ashtouky et al. 2009).

Results and discussion

Characterization of biosynthesized RF-ZnO NPs

The biosynthesized RF-ZnO NPs were confirmed as nanoparticles using UV–Vis, FTIR spectroscopy, BET analysis, SEM, EDAX, HR-TEM, and XRD analysis. Figure 2a displays UV–Vis spectrum of biosynthesized RF-ZnO NPs. Owing to electron transitions from valence to

conduction band of RF-ZnO NPs, the typical absorption peak at 365.35 nm was observed. The band gap of the ZnO catalyst was determined using the Tauc plot method as 3.47 eV. Figure 2b shows the FTIR spectrum of RF-ZnO NPs, illustrating the wavenumbers at 3437, 1635, 1399, 893, and 541 cm^{-1} , respectively. The presence of absorption peaks at 3437 cm^{-1} and 1635 cm^{-1} can be credited to O–H stretching and bending vibrations, respectively. The formation of the target RF-ZnO NPs is confirmed by the FTIR broad absorption feature positioned at 541 cm^{-1} which agrees with stretching vibration of Zn–O (Senthilkumar et al. 2017). The BET surface area and pore size of ZnO nanoparticles were 9.4585 m^2/g and the average pore diameter was 97.30 nm.

Fig. 2 a UV–Vis absorption spectra and b FTIR spectra of RE-ZnO NPs

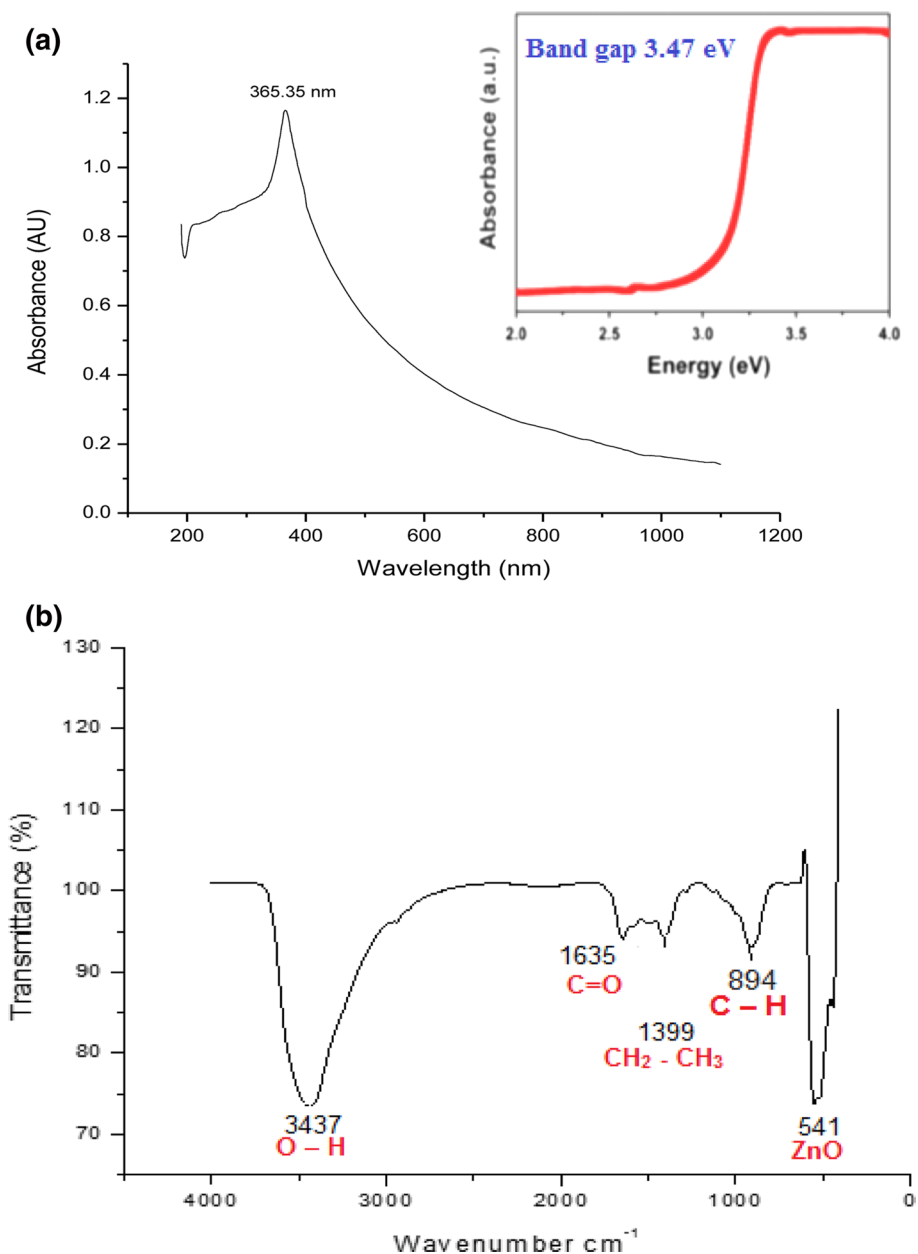
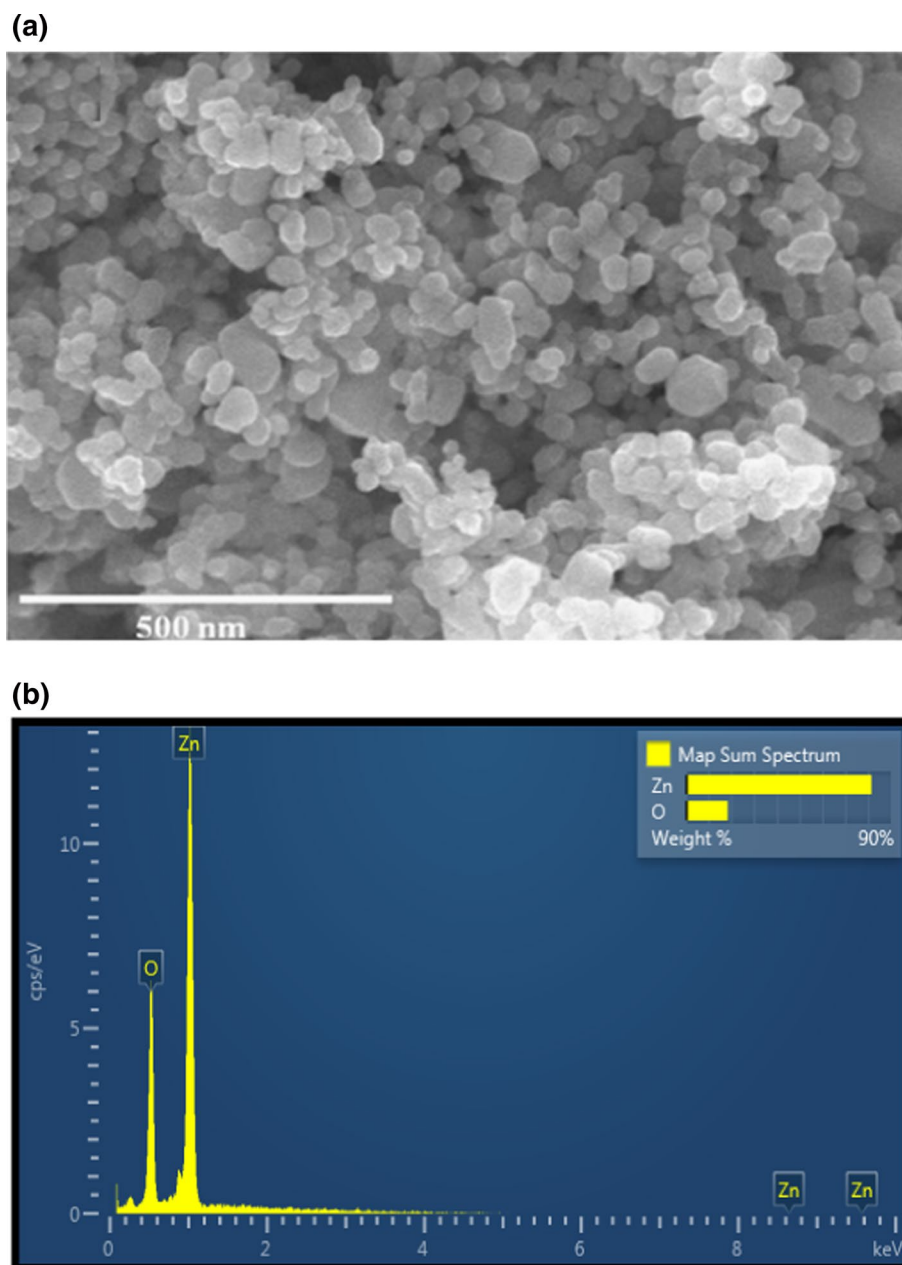


Figure 3a exhibits morphology of green-synthesized RF-ZnO NPs as detected by SEM. It was observed that individual particles aggregated themselves to resemble larger spherical particles, which are uniformly distributed. The RF-ZnO NPs shape was a hexagonal nanochip with a rough surface, and the diameter of the cluster is 2 μm . The chemical composition of RF-ZnO NPs was investigated using EDAX, as shown in Fig. 3b. The EDAX spectrum illustrates existence of Zn and O, composed of carbon and oxygen can be ascribed to the extract and the high value of zinc (90.0%) and oxygen (10.00%), respectively. The synthesized nanoparticles have size range between 1 and 100 nm, and are aggregated into a spherical shape as shown. The results of

the characterization of the RF-ZnO NPs achieved in this present study were found to be analogous to previous investigations on biosynthesis of ZnO NPs using algal and other plant extracts (Azizi et al. 2013); however, this is a novel study on the green synthesis of RF-ZnO NPs by *R. fairholmianus*.

HR-TEM analysis is performed to identify the ZnO NPs morphology, shape, and size (Fig. 4a). It is observed from HR-TEM image that prepared NPs are occurred with size range from 25 to 50 nm. The XRD pattern of green-synthesized RF-ZnO NPs is illustrated in Fig. 4b. The identified peaks match to the ZnO NPs own hexagonal phase and originate in the lattice planes (h, k, l) of (002), (004), (101), (102), (103), (100), (110), (112),

Fig. 3 a SEM image and b EDAX analysis of RE-ZnO NPs



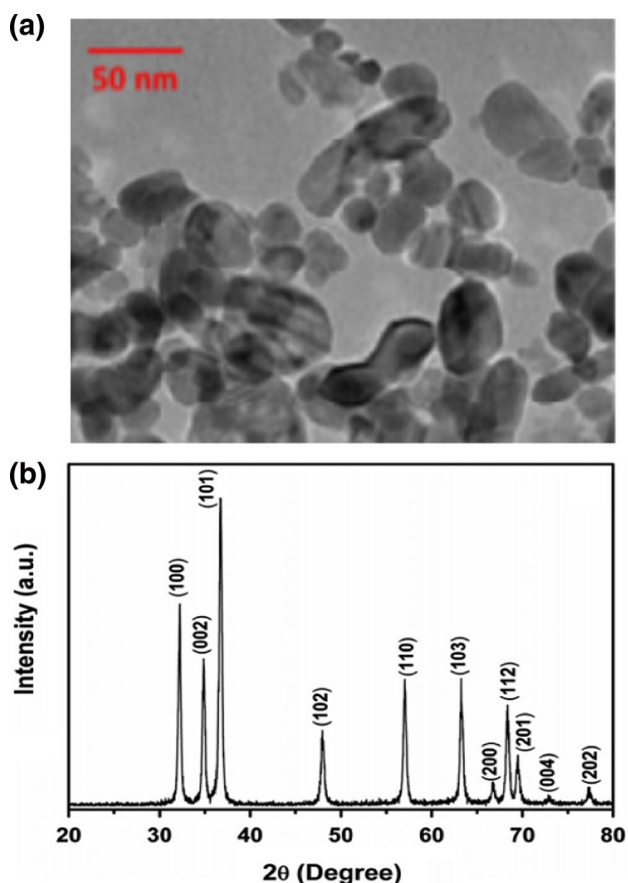


Fig. 4 a HR-TEM image and b XRD pattern of RE-ZnO NPs

(200), (201), and (202) at the following temperatures: 32°, 34°, 36°, 46°, 58°, 64°, 68°, 69°, 70°, 72°, and 78°. The crystalline nature of RF-ZnO NPs was confirmed by the green-synthesized nanoparticle planes (JCPDS card no. 36-1451). The purity of biosynthesized RF-ZnO NPs was confirmed by the result. There were no impurity peaks in the sample. The mean crystalline size of the RF-ZnO NPs calculated from the XRD peaks using Debye–Scherrer’s equation was 11.09 nm.

Table 1 Effect of treatment time and current density on the BPA removal by electrocoagulation process

Electrolysis time (min)	Percentage of BPA removal				
	Current density				
	5 mA cm ⁻²	10 mA cm ⁻²	15 mA cm ⁻²	20 mA cm ⁻²	25 mA cm ⁻²
3	13.78	20.87	22.91	25.67	28.15
6	19.07	25.67	28.15	30.12	31.18
9	22.91	28.15	31.18	34.52	40.77
12	28.15	31.25	42.71	48.90	51.71
15	28.15	34.90	48.90	51.71	54.69
18	31.18	37.50	51.71	54.69	57.32
20	34.18	39.90	54.69	59.83	63.71

Electrocoagulation process (first step)

In the primary step, the sample was treated by electrocoagulation using Al electrodes to eliminate BPA at 20 min of electrolysis under the optimal process parameters. The electrochemical treatment was performed at five current density values: 5, 10, 15, 20, and 25 mA cm⁻² under optimized process variables such as initial pH (7.0), supporting electrolyte (NaCl) concentration (0.05 M), inter-electrode distance (0.5 cm), treatment time (20 min), and stirrer speed (100 rpm). Subsequent to 20 min of treatment, the percentage of BPA removals was 31.18, 39.90, 54.69, 59.83, and 63.71% for current densities of 5, 10, 15, 20, and 25 mA cm⁻², respectively. From Table 1, it can be seen that BPA removal due to electrochemical treatment was greater when current density was also greater. The electrocoagulation mechanisms are elucidated by the fact that at high current, the amount of metal oxidized increases, resulting in a larger amount of precipitate and faster elimination of contaminants (Comminellis and Chen 2011). The maximum BPA removal accomplished was 59.83% after 20 min of electrocoagulation treatment at an optimum current density of 20 mA cm⁻², which was used for the experiments.

Photoelectrocatalytic oxidation process using green-synthesized RF-ZnO nanoparticle (second step)

Application of green-synthesized RF-ZnO NPs was investigated in the photoelectrocatalytic oxidation to achieve complete mineralization of the pretreated BPA solution (electrocoagulation treatment) under RuO₂/IrO₂/TaO₂ coated Ti electrodes. To estimate the effectiveness of the degradation method of BPA, very important parameters viz. initial solution pH of BPA, amount of RF-ZnO NPs, applied current density, and process time were studied. During the photoelectrocatalytic degradation experiments, the BPA concentration and the formation of intermediates were analysed by UV–Vis, HPLC spectrometry, and GC–MS.

Effect of initial pH on BPA degradation rate

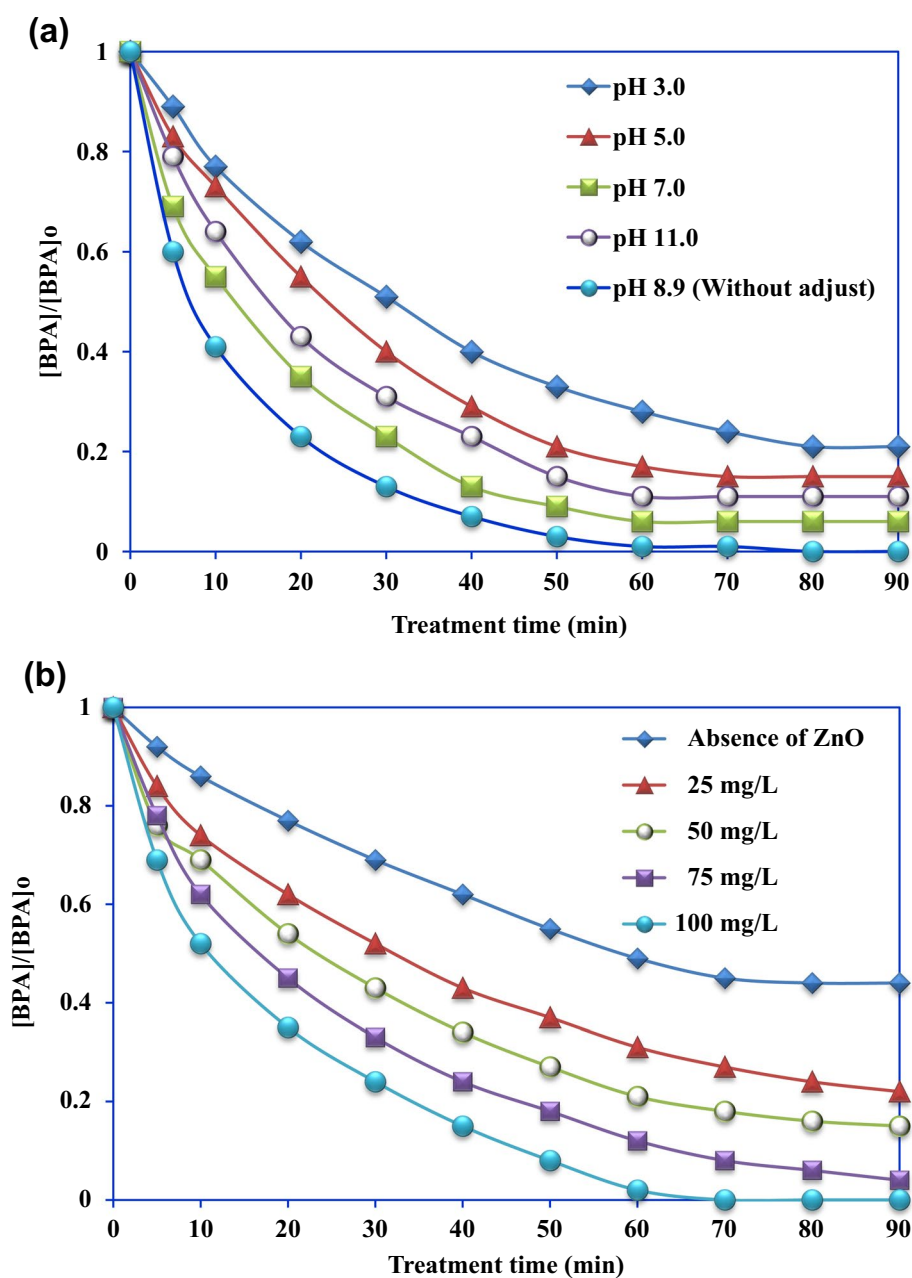
To explore an effect of pH on degradation rate of BPA, tests were performed in 90 min at pH 3, 5, 7, 11, and the original pH 8.2 (after electrocoagulation), with a stirrer speed of 200 rpm and a current density of 20 mA cm^{-2} under UV illumination by photoelectrocatalytic oxidation, and the results are illustrated in Fig. 5a. The result displays that when the sample's original pH of 8.2 was sampled within 90 min treatment process, the degradation rate of BPA increased and reached 100%. However, no significant improvement has been detected when the pH is increased from 8.2 to 11. This is due to the hydrolysis of chlorine yielding the hypochlorite

ion (OCl^-) and hypochlorous acid (HOCl) depending on the solution pH (Majumder et al. 2020). The adsorption capability of the ZnO nanocatalyst under dark environments was identified, and the percentage degradation due to adsorption of ZnO was 18% at 50 mg L^{-1} initial concentration of catalyst at pH 5 for a 90 min reaction time. Therefore, a pH of 8.2 was chosen for successive experiments.

Effect of the RF-ZnO NPs catalyst dosage

The efficiency of photoelectrocatalytic degradation was increased rapidly in association with increasing the catalyst loading at different dosages under the same experimental

Fig. 5 a Effect of pH and b effect of concentration of RE-ZnO NPs [current density applied of 20 mA cm^{-2} and treatment time of 90 min]



conditions (Majumder et al. 2020). Treatment process was carried out in the existence of RF-ZnO NPs catalyst in different dosages of 25, 50, 75, and 100 mg L⁻¹ and in the absence of ZnO NPs at 20 mA cm⁻² and at the original pH of 8.2 (after electrocoagulation treatment) to clarify the effect of RF-ZnO NPs catalyst amount on degradation rate of BPA. As shown in Fig. 5b, increasing the amount of catalyst in different dosages enhanced the BPA degradation rate. When the concentration of the catalyst increased from 25, 50, 75, and 100 mg L⁻¹ of the RF-ZnO NPs, the rate of BPA degradation enhanced considerably, but without catalyst use, there was 44% degradation achieved after 90 min of electrolysis. This was due to increasing the catalyst concentration; ZnO displays higher UV absorption and as a consequence, more capability to break the BPA (Abdul et al. 2021).

Mineralization of BPA occurs due to oxidation of organic pollutants into CO₂ and H₂O by active species like ozone, active chlorine, hydroxide, or hydrogen peroxides that are generated and developed during photocatalytic oxidation on the surface of RF-ZnO NPs simultaneously in direct electrochemical oxidation (Daghrir et al. 2012; Abo et al. 2016). Moreover, ZnO discloses a higher capability to degrade BPA by liberating more free hydroxyl radicals ([•]OH) into the aqueous suspension and as a result, about 100% of degradation could be attained using 100 mg L⁻¹ RF-ZnO NPs after 90 min of degradation. Based on the results, the consequent degradation method was employed by lowest likely catalyst loading in view of the conservation of physical and chemical conditions of water; thus only 75 mg L⁻¹ of the catalysts were used (Nidheesh et al. 2021).

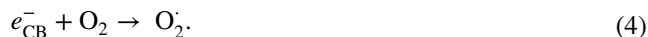
Effect of current densities on BPA degradation

The effectiveness of BBA degradation on photoelectrocatalytic oxidation with respect to current density is depicted in Fig. 6a. As a result, the degradation efficiency increases steadily from 38 to 100% while the applied current density is enhanced from 5 to 25 mA cm⁻², under the experimental conditions such as electrode distance (0.6 cm), stirrer speed (200 rpm), RF-ZnO NPs dosage (75 mg L⁻¹), and initial pH (8.2). It could be ascribed to the increased current density, while the rate of oxidant generation also leads to an increase in degradation rate of BBA. This may be either due to generation of a variety of organic molecules or stable intermediates during the process with oxidation produced during the photoelectrocatalytic oxidation process (Rathinam and Govindaraj 2021).

The photoelectrocatalysis (PEC) mechanism relies on discharge of electron e_{CB}^- on a semiconductor like ZnO from full valence band (VB) to the empty conductive band (CB), producing e_{CB}^-/h_{VB}^+ pairs by the reaction mechanism given below:



The powerful oxidizing photogenerated h_{VB}^+ carry out reactions with adsorbed H₂O to form hydroxyl radical ([•]OH) from reaction (3) whereas the e_{CB}^- react with adsorbed oxygen producing superoxide radical (O₂^{•-}) through reaction (4).



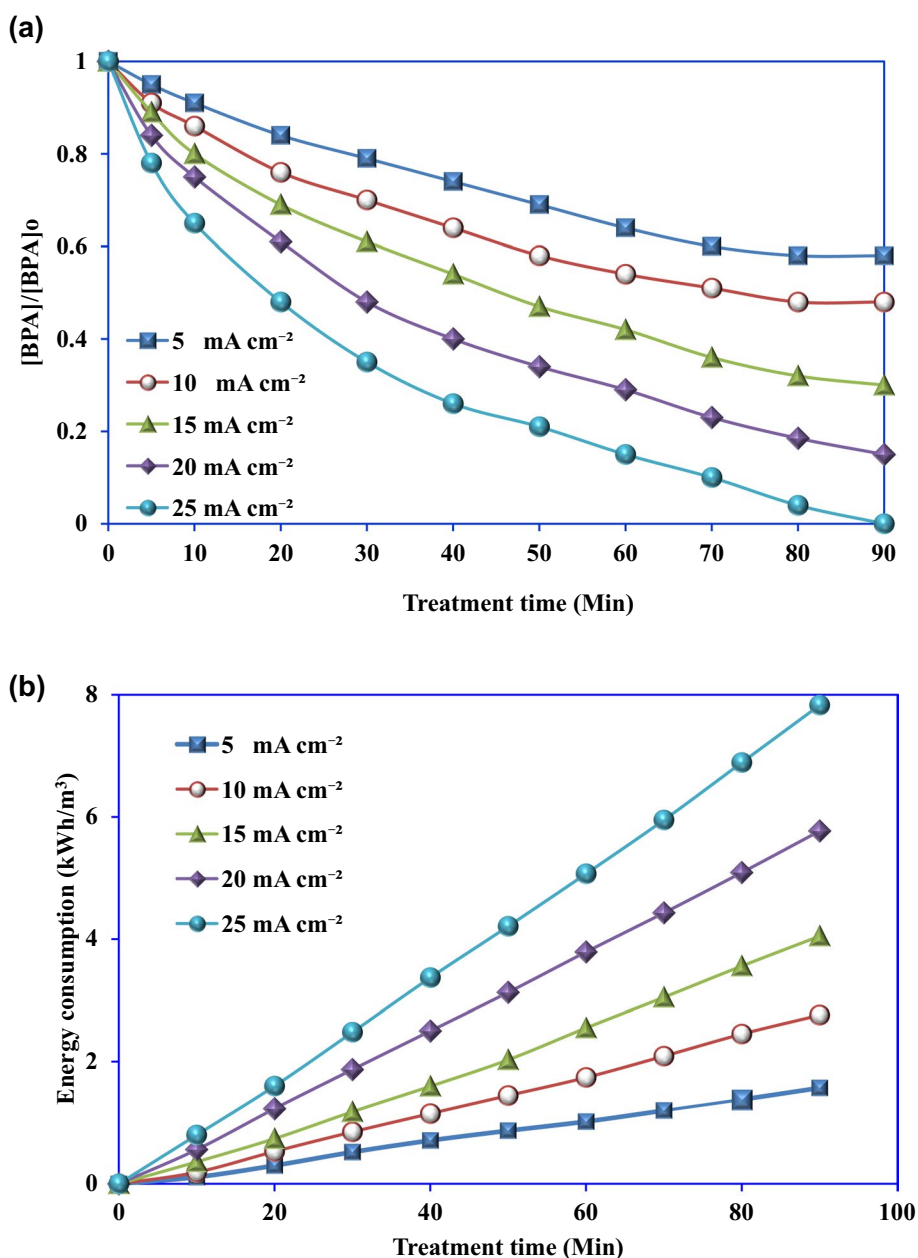
PEC deals with the probability of avoiding recombination of photogenerated e^-/h^+ charge carriers by utilizing bias potential, making it potential for electrons to be portable through external circuit to the counter electrode (Chenah et al. 2021). PEC oxidation activation generates high redox potential radicals namely SO₄^{•-} (2.5–3.1 V) and [•]OH (1.9–2.7 V) (Abdul et al. 2021).

Titanium electrode modified with metal oxide has shown significance improvement in results for the photoelectrocatalytic degradation of BPA. Titanium modified with tin oxide (Ti/SnO₂), lead oxide (Ti/PbO₂), and iridium oxide (Ti/IrO₂) was applied in the treatment of BPA and required 2.0 A cm⁻² to 90% of degraded BPA in solution (Francois et al. 2012). Anodes of titanium electrodes and boron-doped diamond (Ti/DDB), titanium and ruthenium oxide (Ti/RuO₂), titanium with tin oxide and antimony (Ti/Sb-SnO₂) films, and platinum electrode (Pt) mineralized BPA by applying 50 mA cm⁻² for 10 h of electrolysis (Cui et al. 2009). Titanium electrodes modified with tin oxide (Ti/SnO₂) and platinum (Ti/Pt) completely degraded the BPA by applying a current density of 300 mA cm⁻² (Tanaka et al. 2002). Xie and Li (2006) studied PEO of bisphenol-A by using Ti/TiO₂ as an anode. The production of H₂O₂ assisted with the TiO₂ photocatalysis reaction led to a good performance of bisphenol-A degradation.

In this way, the developed anode in this work is very promissory to be used in the BPA photoelectrocatalytic degradation in consequence of its high photocatalytic activity mainly at the first minutes of reaction, using current densities lower than previously reported. The present work is degradation of BPA by titanium (Ti) electrode modified coated with mixed metal oxides (RuO₂/IrO₂/TaO₂) by ZnO NPs using *R. fairholmianus* (RF) root extract. As a result, the complete degradation of BPA, required 25 mA cm⁻², electrode distance (0.6 cm), stirrer speed (200 rpm), RF-ZnO NPs dosage (75 mg L⁻¹), and initial pH (8.2).

Figure 6b shows the energy consumption for the degradation of the BPA as a function of applied current density. The energy consumption enhanced from 1.57 to 7.83 kWh/m³ with respect to increase in the applied current densities from 5 to 25 mA cm⁻² at 90 min. The energy consumption shows

Fig. 6 Effect of applied current density: **a** BPA degradation rate and **b** energy consumption [Initial pH of 8.2 (after 20 min of electrocoagulation), 75 mg L^{-1} of ZnO dosage, and treatment time of 90 min]



an increase when the applied current densities increase by $\text{RuO}_2/\text{IrO}_2/\text{TaO}_2$ coated Ti electrodes using RF-ZnO NPs.

Changes in the UV–visible spectra

Variations in the UV–visible spectra analysis were performed at optimum conditions such as an initial BPA concentration (200 ppm) with NaCl solution (0.1 N) (first stage of electrocoagulation), initial pH (8.2) after 20 min of electrocoagulation, current density (20 mA cm^{-2}), ZnO dosage

(75 mg L^{-1}), and a treatment time (90 min). Along with PEC, aliquots were collected for the spectrometric analysis. The evolution of the UV–visible spectra of the BPA solution before, after, and during the electrocoagulation and PEC treatment processes (Fig. 7). It can be understood that the maximum absorbance peak is at 276 nm, which signifies the BPA, and it was partially reduced after electrocoagulation treatment and completely disappeared later by applying 90 min of PEC treatment processes to $\text{RuO}_2/\text{IrO}_2/\text{TaO}_2$ coated Ti electrodes using RF-ZnO NPs.

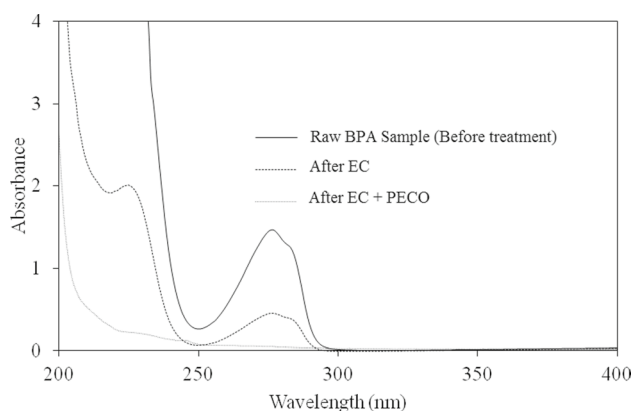


Fig. 7 Changes in the UV–Vis spectra of untreated BPA, after electrocoagulation and after electrocoagulation followed photoelectrocatalytic oxidation processes

HPLC analysis of before and after PEC oxidation treatment

Changes in BPA concentration were measured at various time intervals using HPLC during the PEC oxidation processes at 25 mA cm^{-2} , 75 mg L^{-1} of RE-ZnO NPs dosages. The raw sample indicates a peak at 6.83 min of retention time. For the second sample (the sample obtained after 20 min of PEC oxidation) carried out at 20 mA cm^{-2} peaks areas were shifted to 6.49 min (Supplementary data: Figure S1). After 40 min of treatment time, the peak was shifted to many retention times during the electrochemical degradation. One-ring aromatic compounds, viz. benzoquinone and hydroquinone, have been found as crucial intermediates in the degradation of BPA (Belgn et al. 2003; Cui et al. 2009). In this study, the quantities of hydroquinone and *p*-benzoquinone generated by electrochemical oxidation were similar.

During the electrolysis of BPA from aqueous solution, hydroquinone and benzoquinone could be precursors of polymeric compounds. This was possibly the result of hydroquinone and benzoquinone polymerization on the anodic surface, as it was visibly observed that the solutions were turning light brown and turbid (Inoue et al. 2008). Aromatic rings cleavage in the development of aliphatic acids, such as acetic, maleic, fumaric, and tartaric acids, was observed during the PEC degradation aqueous solution (Cui et al. 2009; Abo et al. 2016). From this result, it is established that BPA was degraded during the PEC oxidation process.

Identification of by-products of photoelectrocatalytic oxidation using GC–MS

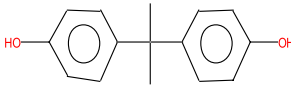
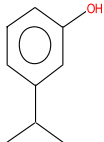
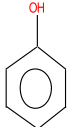
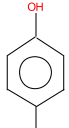
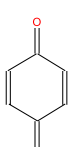
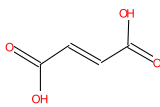
GC–MS analysis was performed for sample collected during the PEC degradation of BPA by $\text{RuO}_2/\text{IrO}_2/\text{TaO}_2$ coated Ti-electrodes using RF-ZnO NPs. Various intermediates were identified by which one was taken. PEC was degraded in 0.1 M NaCl electrolyte at a current density of 25 mA cm^{-2} with an initial BPA concentration of 200 mg L^{-1} . Different ways of degradation of BPA intermediates found out by GC–MS analysis are reported in the supplementary material (Supplementary data: Figure S2).

From the GC analysis, single-ring phenolic compounds were identified as the initial stage of the PEC oxidation. They are presented in Table 2. Isopropylphenol ($m/e = 136$, $\text{tr} = 6.73 \text{ min}$), phenol ($m/e = 94$, $\text{tr} = 5.81 \text{ min}$), benzoquinone ($m/e = 108$, $\text{tr} = 6.17 \text{ min}$), and hydroquinone ($m/e = 110$, $\text{tr} = 6.62 \text{ min}$) have the following retention times (tr). In the PEC oxidation of phenolic compounds, including BPA, aromatic intermediates, hydroxylated BPA, and phenol derivatives, viz. benzoquinone, hydroquinone, hydroxybenzoic acid, resorcinol, catechol, isopropylphenol, and isopropenylphenol have found out. Aromatic cleavage resulting in obtained aliphatic acids has also been investigated with maleic, citric, tartaric, acetic, and formic acids (Belgn et al. 2003; Cui et al. 2009; Abo et al. 2016). Intermediate and by-product results were confirmed and matched with the NIST database. Consequently, as reported by the GC/MS and HPLC examination of intermediate products and present experimental records and literature reports, a probable BPA degradation pathway was construed as illustrated in Scheme 1. The intermediate products present analytical results of PEC oxidation of BPA that are generally coincidence with previous reports. Isopropylphenol and hydroquinone as main by-products for the photoelectrocatalytic oxidation of BPA were also stated by Cui et al. (2009). Other compounds, namely phenol and 2-(4-hydroxyphenyl)-2-propanol, have been found lot as intermediates by Inoue et al. (2008).

Kinetic evaluation

As can be seen from Table 3, the electrocoagulation succeeded by PEC oxidation of BPA follows the kinetics modelling and exhibits a reasonably good fit towards pseudo-first-order kinetics with almost the same rate coefficients (R^2 value) for all the applied current densities (Fig. 8). Utilization of pseudo-first-order reaction kinetic towards PEC oxidation processes at an initial pH of 8.2 (after 20 min of

Table 2 The degradation products during the PEC oxidation identified by GC–MS

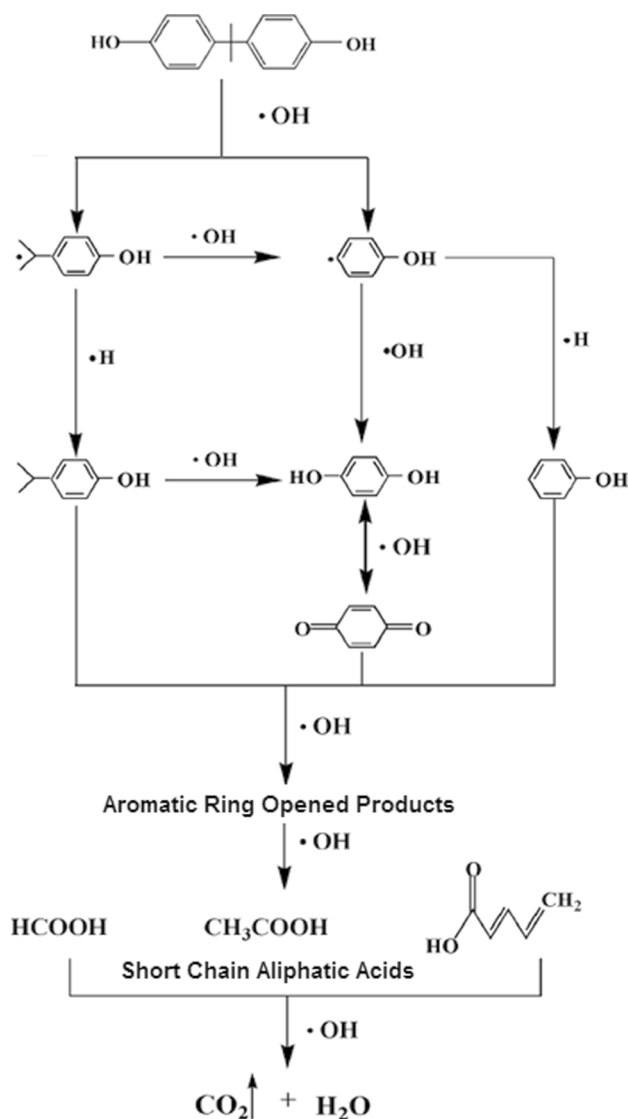
Peak no.	Retention time (min)	Molecular structure	Molecular weight m/z	Chemical names
1	7.03		228	BPA
2	6.73		136	Isopropylphenol
3	5.81		94	Phenol
4	6.62		110	Hydroquinone
5	6.17		108	Benzoquinone
6	5.92		97	2,4-Pentadienic acid
7	4.78	CH ₃ COOH	60	Acetic acid

electrocoagulation), current density of 25 mA cm⁻², 75 mg L⁻¹ of ZnO dosage, and treatment time of 90 min. The graph illustrates the determined rate constant values 2.99, 4.61, 6.9, 8.52, and 11.97 min⁻¹ for the applied current density of 5, 10, 15, 20, and 25 mA cm⁻², respectively.

Conclusions

The application of biosynthesized RF-ZnO NPs in PEC oxidation after electrocoagulation treatment improves the BPA degradation in aqueous solution. The size of biosynthesized RF-ZnO NPs is confirmed by SEM analysis, and its size is 100 nm. In the first stage, the maximum removal of BBA was 59.83%, reached under the optimum parameters of the electrocoagulation process using an Al–Al electrode, current density of 20 mA cm⁻², treatment time of 20 min. Operating variables such as RF-ZnO NPs dosages, initial pH, and current density all had a significant impact on the BPA

degradation rate in the second stages of PEC degradation. Within 90 min treatment process, the complete mineralization of BBA could be attained at 25 mA cm⁻², 75 mgL⁻¹ dosages of RF-ZnO NPs. The HPLC results showed that at the completion of the process, peaks existing as possible characteristics of phenolic compounds viz. catechol, hydroquinone, and BPA degradation products of several acids were identified. Results of this study obviously demonstrate that RF-ZnO NPs have potential application for photocatalysis. The degradation by-products were investigated using GC–MS and the results were confirmed and matched with the NIST database for during the PECO treatment, and a BPA degradation mechanism was also proposed. According to kinetic analysis, the BPA degradation rate may be obeyed as a pseudo-first-order kinetics reaction. It was effectively accomplished to complete removal of BPA in aqueous solution. The novel hybrid electrocoagulation with photoelectrocatalytic oxidation treatment methods of the emerging



Scheme 1 Photoelectrocatalytic degradation pathway of BPA

Fig. 8 Pseudo-first-order kinetics of reaction for BPA removal efficiency on effect of current density [Initial pH of 8.2 (after 20 min of electrocoagulation), 75 mg L⁻¹ of ZnO dosage, and treatment time of 90 min]

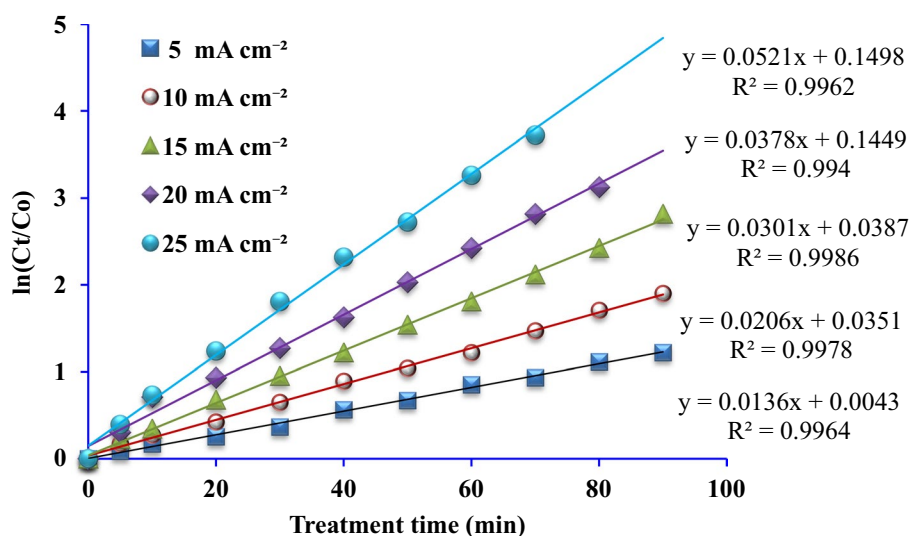


Table 3 Pseudo-first-order rate constants of BPA removal on different current densities by PEC oxidation process

Treatment process	Applied current density (mA/cm ²)	K (min ⁻¹) × 10 ⁻²	R^2
PEC oxidation	5	2.99	0.996
	10	4.61	0.994
	15	6.9	0.998
	20	8.52	0.997
	25	11.97	0.996

pollutant BPA from aqueous solution using titanium (Ti) electrode coated with mixed metal oxides (RuO₂/IrO₂/TaO₂) by green-synthesized ZnO NPs from *R. fairholmianus* root extracts were effectively achieved.

Supplementary Information The online version contains supplementary material available at <https://doi.org/10.1007/s11696-022-02473-w>.

Acknowledgements The authors are intrigued to appreciative for The Management and The Principal of K.Ramakrishnan College of Technology (Autonomous), Samayapuram, Tiruchirappalli-621112, Tamil Nadu, India, for giving fundamental facilities to finish this work.

Authors contribution All authors contributed to the study conception and design. Material preparation, data collection, and analysis were performed by MG, SB, and VV. The first draft of the manuscript was written by RR and KV and all authors commented on previous versions of the manuscript. All authors read and approved the final manuscript.

Funding The authors declare that no funds, grants, or other support were received during the preparation of this manuscript.

Availability of data and materials The data that support the findings of this study are openly available in reference.

Declarations

Conflict of interest The authors have no relevant financial or non-financial interests to disclose.

Ethical approval The submitted work should be original and should not have been published elsewhere in any form or language.

Consent to participate I understand that I will not benefit directly from participating in this research. I agree to my interview being audio-recorded. I understand that all information I provide for this study will be treated confidentially.

Consent to publication I, the undersigned, give my consent for the publication of identifiable details, which can include photograph(s) and/or videos and/or case history and/or details within the text (“Material”) to be published in the above journal and article.

References

- Abdul L, Si X, Sun K, Youbin S (2021) Degradation of bisphenol A in aqueous environment using peroxydisulfate activated with carbonate: performance, possible pathway, and mechanism. *J Environ Chem Eng* 9:105419. <https://doi.org/10.1016/j.jece.2021.105419>
- Abo R, Kummer NA, Merkel BJ (2016) Optimized photodegradation of bisphenol A in water using ZnO, TiO₂ and SnO₂ photocatalysts under UV radiation as a decontamination procedure. *Drink Water Eng Sci* 9:27–35. <https://doi.org/10.5194/dwes-9-27-2016>
- Argote-Fuentes S, Feria-Reyes R, Ramos-Ramírez E, Gutiérrez-Ortega N, Cruz-Jiménez G (2021) Photoelectrocatalytic degradation of congo red dye with activated hydrotalcites and copper anode. *Catalysts* 11:211. <https://doi.org/10.3390/catal11020211>
- Azizi S, Ahmad MB, Namvar F, Mohamad R (2013) Green biosynthesis and characterization of zinc oxide nanoparticles using brown marine macroalga *Sargassum muticum* aqueous extract. *Mater Lett* 116:275–277. <https://doi.org/10.1016/j.matlet.2013.11.038>
- Belgin G, Mehmet AO, Nihaloturan AY (2003) Indirect electrochemical treatment of bisphenol-A in water via electrochemically generated Fenton's reagent. *Environ Sci Technol* 37:3716–3723. <https://doi.org/10.1021/es034011e>
- Chennah A, Amaterz E, Taoufiq A, Bakiz B, Kadmi Y, Bazzi L, Guinneton F, Gavarrri J-R, Benlhachemi A (2021) Photoelectrocatalytic degradation of Rhodamine B pollutant with a novel zinc phosphate photoanode. *Process Saf Environ Prot* 148:200–209. <https://doi.org/10.1016/j.psep.2020.10.012>
- Comninellis C, Chen G (2011) *Electrochemistry for the environment*. Springer, New York
- Cui YH, Li XY, Chen GH (2009) Electrochemical degradation of bisphenol A on different anodes. *Water Res* 43:1968–1976. <https://doi.org/10.1016/j.watres.2009.01.026>
- Daghrir R, Drogui P, Robert D (2012) Photoelectrocatalytic technologies for environmental applications. *J Photochem Photobiol A Chem* 238:41–52. <https://doi.org/10.1016/j.jphotochem.2012.04.009>
- El-Ashtouky E-SZ, Amin NK, Abdelwahab O (2009) Treatment of paper mill effluents in a batch-stirred electrochemical tank reactor. *Chem Eng J* 146:205–210. <https://doi.org/10.1016/j.cej.2008.05.037>
- Francois Z, Drogui P, Blais J-F, Mercier G (2012) Electrochemical treatment of bisphenol-A using response surface methodology. *J Appl Electrochem* 42:95–109. <https://doi.org/10.1007/s10800-011-0376-y>
- Goulart LA, Alves SA, Mascaro LH (2019) Photoelectrochemical degradation of bisphenol A using Cu doped WO₃ Electrodes. *J Electroanal Chem* 839:123–133. <https://doi.org/10.1016/j.jelechem.2019.03.027>
- Govindaraj M, Pattabhi S (2015) Electrochemical treatment of endocrine-disrupting chemical from aqueous solution. *Desalin Water Treat* 53:2664–2674. <https://doi.org/10.1080/19443994.2013.868834>
- Govindaraj M, Amrita S, Sukumar C, Hariprakash B, Pattabhi S (2012) Treatment of endocrine disrupting chemical from aqueous solution by electrocoagulation. *Sep Sci Technol* 48:295–302. <https://doi.org/10.1080/01496395.2012.686001>
- Govindaraj M, Rathinam R, Sukumar C, Uthayasankar M, Pattabhi S (2013) Electrochemical oxidation of bisphenol-A from aqueous solution using graphite electrodes. *Environ Technol* 34:503–511. <https://doi.org/10.1080/09593330.2012.701333>
- Inoue M, Masuda Y, Okada F, Sakurai A, Takahashi I, Sakakibara M (2008) Degradation of bisphenol A using sonochemical reactions. *Water Res* 42:1379–1386. <https://doi.org/10.1016/j.watres.2007.10.006>
- Ju P, Fan H, Guo D, Meng X, Xu M, Ai S (2012) Electrocatalytic degradation of bisphenol A in water on a Ti-based PbO₂-ionic liquids (ILs) electrode. *Chem Eng J* 179:99–106. <https://doi.org/10.1016/j.cej.2011.10.065>
- Kang JH, Kondo F, Katayama Y (2006) Human exposure to bisphenol A. *Toxicology* 226:79–89. <https://doi.org/10.1016/j.tox.2006.06.009>
- Koby M, Gebologlu U, Ulu F, Oncel S, Demirbas E (2011) Removal of arsenic from drinking water by the electrocoagulation using Fe and Al electrodes. *Electrochim Acta* 56:5060–5070. <https://doi.org/10.1016/j.electacta.2011.03.086>
- Laxma PV, Ki-H K, Kavitha B, Kumar V, Raza N, Kalagara S (2018) Photocatalytic degradation of bisphenol A. *Rev J Environ Manag* 213:189–205. <https://doi.org/10.1016/j.jenvman.2018.02.059>
- Majumder S, Chatterjee S, Basnet P, Mukherjee J (2020) ZnO based nanomaterials for photocatalytic degradation of aqueous pharmaceutical waste solutions: a contemporary review. *Environ Nanotechnol Monit Manag* 14:100386. <https://doi.org/10.1016/j.enmm.2020.100386>
- Moodley JS, Krishna SBN, Serphen KP, Govender P (2018) Green synthesis of silver nanoparticles from *Moringa oleifera* leaf extracts and its antimicrobial potential. *Adv Nat Sci Nanosci Nanotechnol* 9:015011. <https://doi.org/10.1088/2043-6254/aaabb2>
- Nidheesh PV, Scaria J, Babu DS, Suresh Kumar M (2021) An overview on combined electrocoagulation-degradation processes for the effective treatment of water and wastewater. *Chemosphere* 263:1279070. <https://doi.org/10.1016/j.chemosphere.2020.127907>
- Qu X, Alvarez PJJ, Li Q (2013) Applications of nanotechnology in water and wastewater treatment. *Water Res* 47:3931–3946. <https://doi.org/10.1016/j.watres.2012.09.058>
- Rajendran NK, George BP, Houreld NN, Abrahamse H (2021) Synthesis of zinc oxide nanoparticles using *Rubus fairholmianus* root extract and their activity against pathogenic bacteria. *Molecules* 26:3029. <https://doi.org/10.3390/molecules26103029>
- Rathinam R, Govindaraj M (2021) Photoelectrocatalytic oxidation of textile industry wastewater by RuO₂/IrO₂/TaO₂ coated titanium electrodes. *Nat Environ Pollut Technol* 20:1069–1076. <https://doi.org/10.46488/NEPT.2021.v20i03.014>
- Senthilkumar N, Nandhakumar E, Priya P, Soni C, Vimalan M, Vetha N (2017) Synthesis of ZnO nanoparticles using leaf extract of *Tectona grandis* (L.) and their anti-bacterial, anti-arthritis, anti-oxidant and in vitro cytotoxicity activities. *New J Chem* 41:10347–10356. <https://doi.org/10.1039/C7NJ02664A>
- Staples CA, Dorn GM, Klecka ST, O'Block HLR (1998) A review of the environmental fate, effects and exposures of bisphenol

- A. Chemosphere 36:2149–2173. [https://doi.org/10.1016/s00456535\(97\)10133-3](https://doi.org/10.1016/s00456535(97)10133-3)
- Tanaka S, Nakata Y, Kimura T, Kawasaki M, Kuramitz H (2002) Electrochemical decomposition of bisphenol A using Pt/Ti and SnO₂/Ti anodes. J Appl Electrochem 32:197–201. <https://doi.org/10.1023/A:1014762511528>
- Xie Y-B, Li XZ (2006) Degradation of bisphenol A in aqueous solution by H₂O₂-assisted photoelectrocatalytic oxidation. J Hazard Mater B138:526–533. <https://doi.org/10.1016/j.jhazmat.2006.05.074>
- Zheng Y, Li F, Fuigui H, Aiwu W, Wen C, Jinping Y, Feng P (2015) Green biosynthesis and characterization of zinc oxide nanoparticles using *Corymbia citriodora* leaf extract and their photocatalytic activity. Green Chem Lett Rev 8:59–63. <https://doi.org/10.1080/17518253.2015.1075069>

Publisher's Note Springer Nature remains neutral with regard to jurisdictional claims in published maps and institutional affiliations.

Springer Nature or its licensor holds exclusive rights to this article under a publishing agreement with the author(s) or other rightsholder(s); author self-archiving of the accepted manuscript version of this article is solely governed by the terms of such publishing agreement and applicable law.